

RESEARCH

Open Access



Retinal optical coherence tomography intensity spatial correlation features as new biomarkers for confirmed Alzheimer's disease

Zi Jin^{1,2,3†}, Xinmin Wang^{1,2,3†}, Ying Lang^{4†}, Yufeng Song^{1,2,3}, Huangxiong Zhan^{1,2,3}, Wuge Shama^{1,2,3}, Yingying Shen⁴, Guihua Zeng⁴, Faying Zhou⁴, Hongjian Gao^{1,2,3}, Shuling Ye^{1,2,3}, Yanjiang Wang⁴, Fan Lu^{1,2,3*} and Meixiao Shen^{1,2,3*}

Abstract

Background The nature and severity of Alzheimer's disease (AD) pathologies in the retina and brain correspond. However, retinal biomarkers need to be validated in clinical cohorts with confirmed AD biomarkers and optical coherence tomography (OCT). The main objective of this study was to investigate whether retinal metrics measured by OCT aid in the early screening and brain pathology monitoring for confirmed AD.

Methods This was a case–control study. All participants underwent retinal OCT imaging, and neurological examinations, including amyloid- β (A β) positron emission tomography. Participants were subdivided into cognitively normal (CN), mild cognitive impairment (MCI), and AD-derived dementia (ADD). Except retinal thickness, we developed the grey level co-occurrence matrix algorithm to extract retinal OCT intensity spatial correlation features (OCT-ISCF), including angular second matrix (ASM), correlation (COR), and homogeneity (HOM), one-way analysis of variance was used to compare the differences in retinal parameters among the groups, and to analyze the correlation with brain A β plaques and cognitive scores. The repeatability and robustness of OCT-ISCF were evaluated using experimental and simulation methods.

Results This study enrolled 82 participants, subdivided into 20 CN, 22 MCI, and 40 ADD. Compared with the CN, the thickness of retinal nerve fiber layer and myoid and ellipsoid zone were significantly thinner ($P < 0.05$), and ASM, COR, and HOM in several retinal sublayers changed significantly in the ADD ($P < 0.05$). Notably, the MCI showed significant differences in ASM and COR in the outer segment of photoreceptor compared with the CN ($P < 0.05$). The changing pattern of OCT-ISCF with interclass correlation coefficients above 0.8 differed from that caused by speckle noise, and was affected by OCT image quality index. Moreover, the retinal OCT-ISCF were more strongly correlated with brain A β plaque burden and MoCA scores than retinal thickness. The accuracy using retinal OCT-ISCF (AUC = 0.935, 0.830) was better than that using retinal thickness (AUC = 0.795, 0.705) in detecting ADD and MCI.

[†]Zi Jin, Xinmin Wang and Ying Lang contributed equally to the work presented here and should therefore be regarded as equivalent authors.

*Correspondence:

Fan Lu
lufan62@mail.eye.ac.cn
Meixiao Shen
smx77@mail.eye.ac.cn

Full list of author information is available at the end of the article



Conclusions The study demonstrates that retinal OCT-ISCF enhance the association and detection efficacy of AD pathology compared to retinal thickness, suggesting retinal OCT-ISCF have the potential to be new biomarkers for AD.

Keywords Alzheimer's disease, Early warning, Retina, OCT, Texture features

Introduction

Alzheimer's disease (AD), a progressive neurodegenerative disease, is the most common cause of dementia. Before the clinical symptoms, brain pathological changes in the AD, such as amyloid beta (Aβ) plaques and phosphorylated tau, have occurred. Currently, AD treatments can slow the progression of the disease instead of curing it, making early screening and intervention for AD important. At present, positron emission tomography (PET) and cerebrospinal fluid (CSF) examinations are the gold standard for diagnosing AD. However, the above

examinations are not widely used for early screening and progression monitoring because they are invasive and non-portable [1–3]. As the extension of the central nervous system, the retina shares similar cellular structure, immune response, and microvascular circulation characteristics to the brain [4]. More importantly, the retina exhibits AD-specific pathological changes, including Aβ deposits, and common effects of AD on both retina and brain are reported during disease progression and in response to therapy (Fig. 1A). In addition, retinal imaging is a non-invasive, portable, quick, and cost-effective tool.

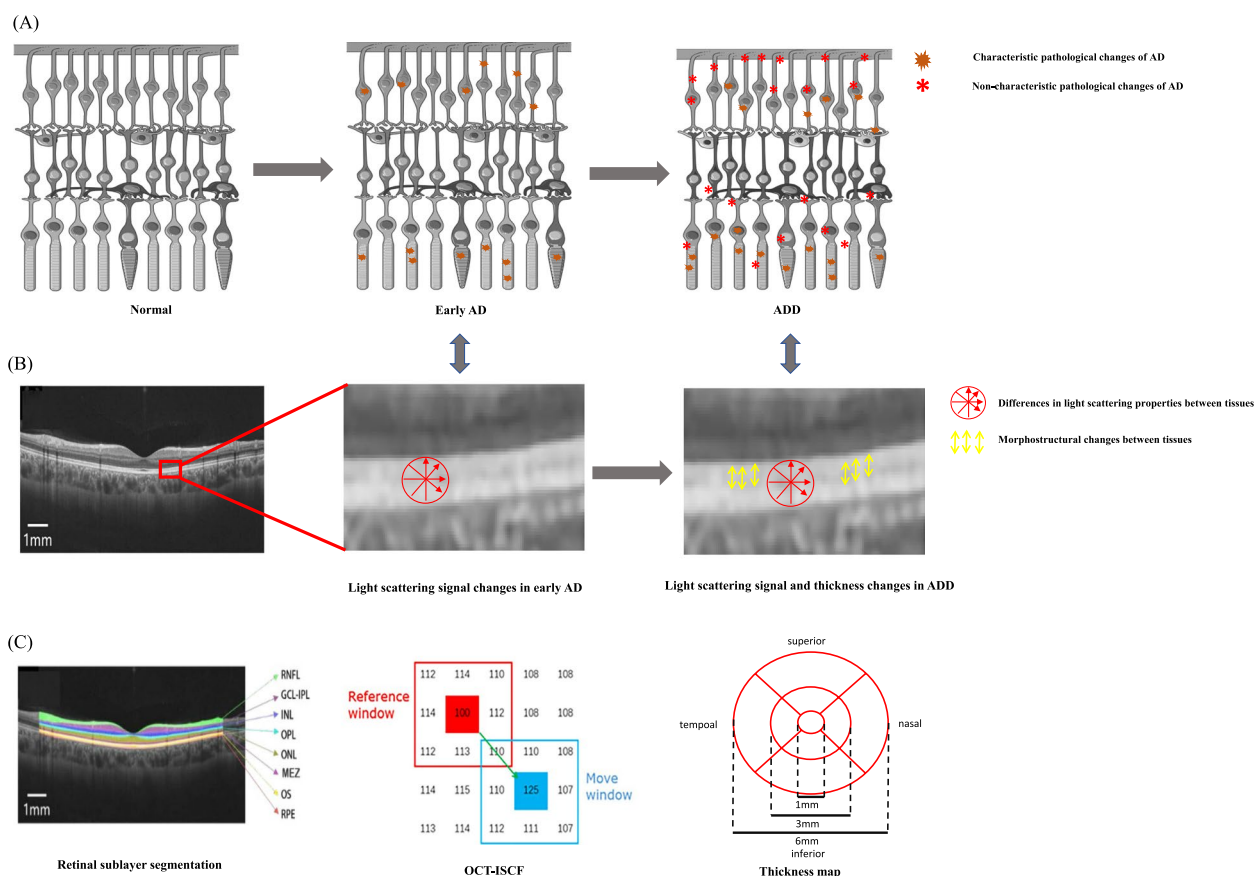


Fig. 1 Schematic diagram of retinal pathological changes in AD based on retinal OCT imaging features. **A** Retinal pathological changing patterns from normal to AD-derived dementia (ADD). **B** The correspondence between retinal pathological changes and OCT imaging features in AD, such as optical scattering property and structural morphology. **C** Retinal OCT imaging features quantization metrics, including OCT intensity spatial correlation features (OCT-ISCF) and thickness in different retinal sublayers. GCIPL, ganglion cells and inner plexiform layer; INL, inner nuclear layer; MEZ, myoid and ellipsoid zone; ONL, outer nuclear layer; OPL, outer plexiform layer; OS, outer segment of photoreceptor; RNFL, retinal nerve fiber layer; RPE, retinal pigment epithelium. This figure contains modified images from Servier Medical Art (<https://smart.servier.com>) licensed by a Creative Commons Attribution 3.0 Unported License

Therefore, the retina has the potential to be a detection window for early screening and progression monitoring in AD.

Optical coherence tomography (OCT) is a non-invasive, widespread technique with high axial resolution, which can obtain in vivo retinal imaging results consistent with histological staining to assess the degree of retinal neurodegeneration [5, 6]. Based on OCT, most studies have found retinal thickness alterations in AD [7], and it is significantly related to the neurodegeneration in the brain [8, 9]. However, many studies have reported that the retinal thickness increases due to glial hyperplasia in the early stage of AD [10, 11], while it decreases significantly in the advanced stage of AD caused by neurodegeneration [12]. To some extent, the high overlap between early AD and healthy individuals occurs due to the fluctuating altered characteristics of the retinal thickness. In other words, the retinal thickness lacks high sensitivity for early AD, and will be limited in early screening.

Recently, several studies have reported AD specific pathological biomarkers, such as A β , can affect the optical scattering properties of tissues near the deposition area, causing changes of reflection spectrum [13, 14]. Moreover, AD non-specific pathological changes, including retinal neurodegeneration, also cause changes in optical scattering properties [15]. Since A β deposition occurs earlier than neurodegeneration [16], the changes in retinal optical scattering properties are thought to precede the changes in retinal thickness (Fig. 1B). In general, the OCT intensity correlates with the tissular optical scattering properties [17–19]. Considering the localized diffuse nature of AD pathological alterations, OCT intensity spatial correlation features (OCT-ISCF) may detect subtle alteration in OCT intensity [20]. The OCT-ISCF are high-order structural features, characterizing the spatial correlation distribution of OCT intensity signal [21, 22]. To the best of our knowledge, there are no studies to confirm the feasibility of retinal OCT-ISCF for early screening and brain pathology monitoring in confirmed AD.

In the present work, we first developed a retinal sub-layer feature extraction algorithm to obtain OCT-ISCF, and compared the detection performance of OCT-ISCF and retinal thickness in different stages of AD. The repeatability and robustness of OCT-ISCF were also evaluated using experimental and simulation methods. Further, we explored the association between retinal metrics and brain pathological changes in AD.

Methods

Participants

The study was approved by the Ethics Committee of the Third Affiliated Hospital of the PLA Army Medical

University (Approval No. 2020–14) and the Affiliated Eye Hospital of Wenzhou Medical University (Approval No. 2020–012-K-10) in accordance with the principles of the Declaration of Helsinki, and written informed consent from all participants were obtained. This project has been registered in the Chinese Clinical Trials Registry (registration number: ChiCTR2000040786; registration date: 2020–12-10). From December 2020 to December 2023, 82 subjects were enrolled by a neurologist (Y.W.) in the Memory Disorders Clinic. All subjects underwent neurological examinations, routine ophthalmological examinations and retinal OCT imaging, which were described in eMethods in the Supplement. When collecting eye data for each patient, we tried to collect both eyes as much as possible, but considering the correlation of binocular data, only one eye data was analyzed in subsequent image analysis, and the right eye data was preferentially included. If the OCT image quality of the right eye is poor (image quality index less than 7 or image discontinuity), the left eye is selected. According to the National Institute of Aging and Alzheimer's Association (NIA-AA) criteria, 62 patients with AD were diagnosed using brain A β -PET results. Based on Clinical Dementia Rating Scale (CDR), AD patients were subdivided into 40 patients with ADD and 22 patients with mild cognitive impairment (MCI) [23]. Twenty cognitively normal (CN) age- and sex-matched subjects with A β -PET negative were recruited.

Exclusion criteria: (1) History of retinal disease, ocular trauma, severe cataract, and high myopia/astigmatism; (2) Dementia not caused by AD, such as Parkinson's dementia, and vascular dementia; (3) The retinal OCT image quality index is less than 7.

Analysis of retinal thickness parameters

All retinal OCT images were analyzed by a custom-built deep learning segmentation algorithm [24]. In Fig. 1C, the retinal image is divided into 8 layers, which are retinal nerve fiber layer (RNFL), ganglion cells and inner plexiform layer (GCIPL), inner nuclear layer (INL), outer plexiform layer (OPL), outer nuclear layer (ONL), myoid and ellipsoid zone (MEZ), outer segment of photoreceptor (OS) and retinal pigment epithelium (RPE), respectively [25]. The average thickness of 8 retinal sublayers in the Early Treatment Diabetic Retinopathy Study (ETDRS) grid was measured.

Analysis of retinal OCT-ISCF and performance test

The gray level co-occurrence matrix (GLCM) algorithm was developed to extract retinal OCT-ISCF [26, 27]. The OCT-ISCF contained angular second order moment (ASM), contrast (CON), correlation (COR), homogeneity (HOM) and dissimilarity (DIS). Detailed

calculations of the OCT-ISCF were described in the supplementary material (eMethods). We performed a small-scale study of retinal OCT-ISCF repeatability on 21 young healthy volunteers. Each subject had two repeated retinal OCT imaging acquisitions by the same operator using the same OCT scan protocol. The same performer analyzed the retinal OCT images to obtain the OCT-ISCF of full-layer retina. In addition, we took pre- and postoperative OCT images of 10 patients who underwent cataract surgery, to investigate the influence of OCT image quality index on the OCT-ISCF. Speckle noise usually occurs in OCT images and is represented as a scattered highlighted signal [28, 29]. To test the robustness of retinal OCT-ISCF for early detection of AD, we randomly added several highlighted signals to retinal OCT images of 5 CN subjects to simulate speckle noise. Subsequently, we analyzed the changes in OCT-ISCF before and after the addition of simulation noise.

Statistical analysis

All statistical analyses were performed by the SPSS 25. The measurement data were presented in the form of mean (standard deviation). The interclass correlation coefficient (ICC) was calculated to assess the repeatability of retinal OCT-ISCF. Shapiro–Wilk was used to test the normal distribution of data. One-way analysis of variance and Bonferroni post hoc test were used to test the measured values of normal distribution. If none of the three groups of data conforms to the normal distribution, the Kruskal–Wallis non-parametric test. Categorical variables were analyzed by chi-square test. Paired t-tests were used to analyze the variability of OCT-ISCF before and after cataract surgery, and speckle noise addition. Correlations of retinal metrics with brain Aβ plaque burden and Montreal Cognitive Assessment (MoCA) scores were analyzed by age-adjusted partial correlation analysis. The stepwise multivariate binary logistic regression analysis and receiver operating characteristics (ROC) curve were used to identify MCI and ADD by retinal thickness and OCT-ISCF, respectively. $P < 0.05$ was considered statistically significant.

Results

In this study, 82 subjects were subdivided into 40 ADD, 22 MCI and 20 CN. The basic demographics and ocular parameters of three groups are summarized in Table 1. There were no significant differences in above parameters, except for MoCA and CDR scores. The MoCA and CDR scores of ADD were lower than those of MCI, which were lower than those of CN.

Table 1 Clinical characteristics of subjects among CN, MCI, and ADD

Characteristics	CN (n=20)	MCI (n=22)	ADD (n=40)	P Value
Sex, No. (%)				
Male	6 (30)	11 (50)	15 (37)	0.40
Female	14 (70)	11 (50)	25 (62)	
Age, mean (SD), y	62.2 (6.2)	65.7 (8.3)	64.5 (7)	0.36
OCT image quality index	8.1 (0.8)	7.9 (0.8)	8.1 (0.9)	0.71 [‡]
Hypertension, No. (%)	6 (30)	4 (18)	8 (20)	0.66
Diabetes, No. (%)	3 (15)	3 (13)	4 (10)	0.86
SE (D)	−0.8 (1.3)	−0.3 (2.0)	0.6 (1.1)	0.06
BCVA (logMAR)	0.04 (0.10)	0.05 (0.09)	0.05 (0.12)	0.88
IOP (mmHg)	15.7 (2.6)	15.1 (2.6)	15.2 (3.1)	0.77
MoCA	23.5 (2.9) ^{b,c}	17.0 (4.6) ^{a,c}	9.3 (4.7) ^{a,b}	< 0.001*
CDR	0 ^{b,c}	0.5 ^{a,c}	1.3 (0.6) ^{a,b}	< 0.001 ^{‡*}

Abbreviations: BCVA best corrected visual acuity, CDR Clinical Dementia Rating Scale, IOP Intraocular pressure, MoCA Montreal Cognitive Assessment, SD standard deviation, SE spherical equivalent refraction

^a Statistical difference with CN group

^b Statistical difference with MCI group

^c Statistical difference with ADD group;

[‡] chi-square test

* $P < 0.05$

Differences in retinal thickness among groups

eTable 1 shows the thickness of each retinal sublayers in three groups according to ETDRS grid. Compared with CN, the RNFL and MEZ in the outer inferior region and the MEZ in the inner temporal region reduced significantly only in the ADD ($P < 0.05$). Compared with the MCI, the ADD showed significant thinning of RNFL in the inferior region and OPL in the outer superior and temporal regions ($P < 0.05$).

Retinal OCT-ISCF performance test and differences among groups

In eTable 2, ICCs of all retinal OCT-ISCF are greater than 0.8. eFigure 1 shows all retinal OCT-ISCF are significantly altered before and after surgery. eTable 3 summarizes retinal OCT-ISCF in various retinal sublayers among three groups. Figure 2 shows that compared with CN, ASM in GCIPL, INL, OPL, OS and RPE sublayers, COR in GCIPL, OPL, OS and RPE sublayers, and HOM in OPL and OS sublayers in ADD varies significantly ($P < 0.05$). It is worth noting that there were also significant differences in ASM and COR in OS sublayer between CN and MCI ($P < 0.05$). In eFigure 2, the results show that the CON, COR, and HOM increase significantly after speckle noise addition, while the ASM decreases significantly. In contrast, the change pattern in

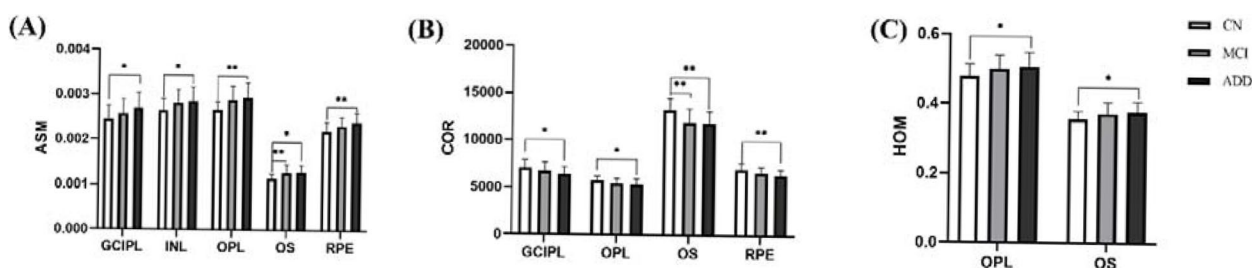


Fig. 2 OCT-ISCF parameters with statistical differences among groups. (A-C) stands for ASM, COR, and HOM parameters respectively. (ASM, angular second moment; COR, correlation; GCIPL, ganglion cells and inner plexiform layer, HOM, homogeneity; INL, inner nuclear layer; OPL, outer plexiform layer; OS, outer segment of photoreceptor; RPE, retinal pigment epithelium; *, $P < 0.05$; **, $P < 0.01$)

OCT-ISCF between AD and CN showed increased ASM and decreased COR, which was opposite to those of adding speckle noise.

Diagnostic performance of retinal metrics for different stages of AD

Figure 3 provides the diagnostic performance of retinal metrics for different stages of AD using ROC analysis. To discriminate ADD from CN, the thickness parameters of RNFL, OPL, MEZ, and RPE were included in a multi-variate model with area under the curve (AUC) of 0.795, while the OCT-ISCF parameters COR of the RNFL, GCIPL, INL, and RPE sublayers, the ASM of the RNFL, GCIPL, and OPL sublayers, and HOM of OS sublayers were included in another multi-variate model with AUC of 0.935 (Fig. 3A). To discriminate MCI from CN, the thickness parameters of the MEZ and RPE were included in a multi-variate model with AUC of 0.705, while the COR of the retina full-layer, GCIPL, INL, OPL, MEZ

sublayers, and ASM of the OPL and MEZ were included in the analysis with AUC of 0.830 (Fig. 3B).

Significant correlation of retinal metrics with brain Aβ plaque burden and cognitive function

Figure 4 presents correlation coefficients of brain Aβ plaque burden and MoCA scores with retinal sublayers thickness in ETDRS grid and OCT-ISCF. Specifically, there were significant correlations between retinal sublayers thickness with standardised uptake value ratio (SUVr) in different brain regions. The above correlation coefficients ranged from -0.318 to 0.362 (Fig. 4A). Moreover, there also were significant correlations between SUVr in different brain regions and retinal OCT-ISCF in several sublayers. Of note, the correlation coefficients between retinal OCT-ISCF and brain SUVr ranged from -0.494 to 0.40 (Fig. 4B).

There were also significant correlations of MoCA scores with retinal sublayer thickness and OCT-ISCF. In terms of retinal thickness, MoCA scores were

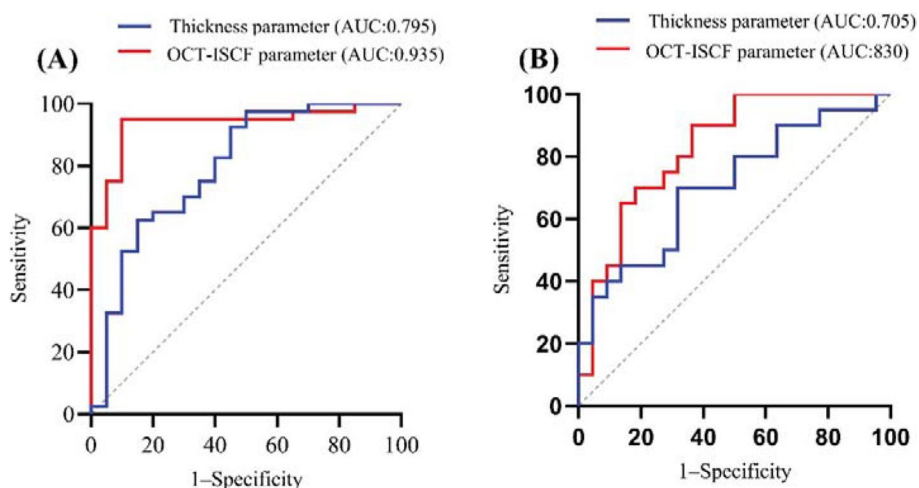


Fig. 3 The differential efficacy of retinal thickness and OCT-ISCF parameters between groups. **A** The ROC curves of Retinal thickness and OCT-ISCF parameters identify ADD and CN; **B** The ROC curves of Retinal thickness and OCT-ISCF parameters identify MCI and CN

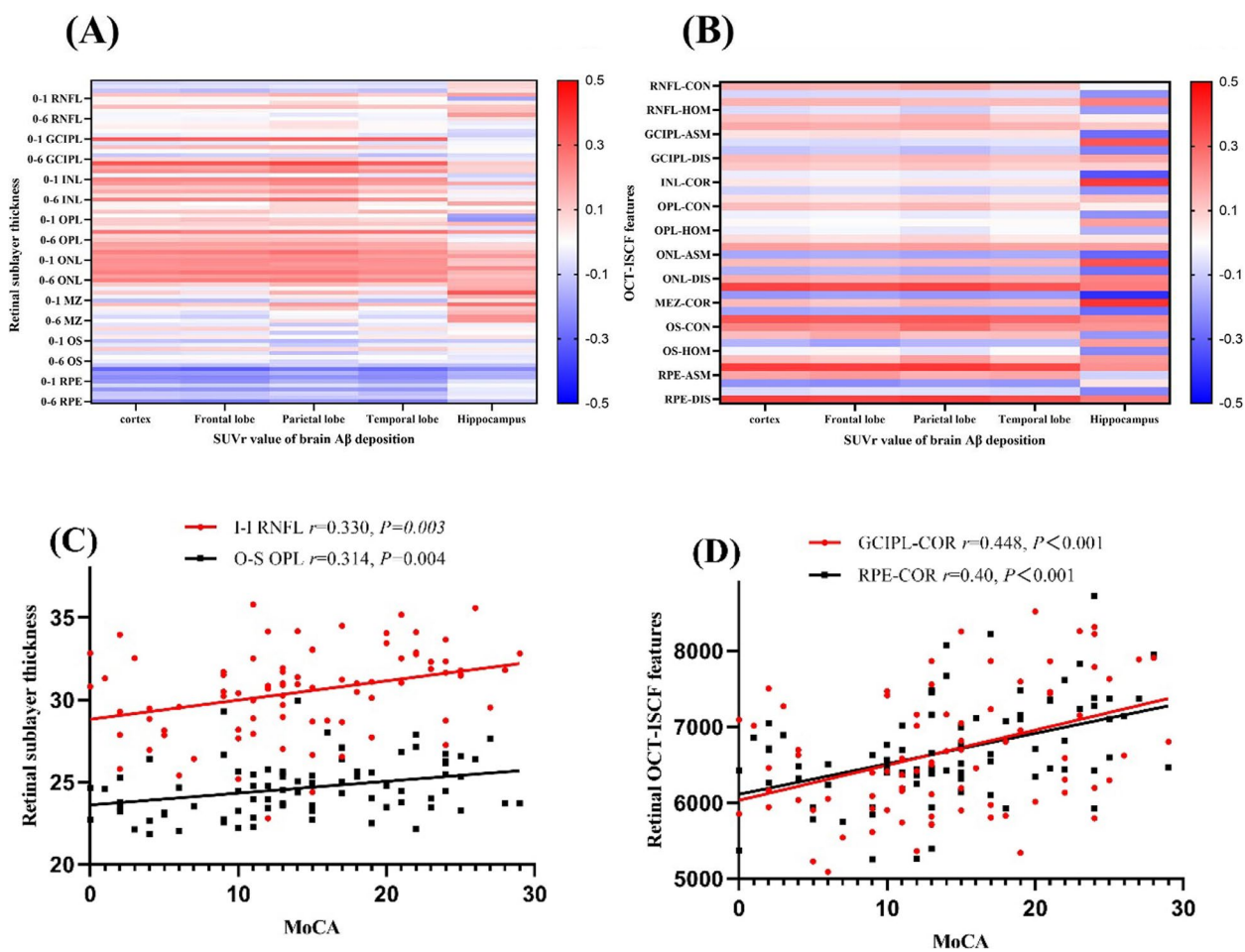


Fig. 4 Correlation of retinal sublayers thickness and OCT-ISCF parameters with brain Aβ-SUVr values and MoCA scores. **A** The retinal sublayers thickness in ETDRS grid were correlated with the SUVr in different brain regions; **B** The retinal sublayers OCT-ISCF were correlated with the SUVr in different brain regions; **C** The correlation between retinal thickness parameters and MoCA scores; **D** The correlation between retinal OCT-ISCF and MoCA scores. (COR, correlation; GCIPL, ganglion cells and inner plexiform layer; I-I, inner-inferior; OPL, outer plexiform layer; O-S, outer-superior; RNFL, retinal nerve fiber layer; RPE, retinal pigment epithelium; SUVr, standardised uptake value ratio

significantly correlated with RNFL, GCIPL, INL, OPL and MEZ sublayers. Specifically, the highest correlation between retinal thickness and MoCA scores in the inner retina was the RNFL sublayer ($r=0.330, P=0.003$), and that in the outer retina was the OPL sublayer ($r=0.314, P=0.004$) (Fig. 4C). Moreover, there were significant correlations between MoCA scores and retinal OCT-ISCF in the RNFL, GCIPL, INL, OPL, OS, and RPE sublayers, with the highest correlation between the GCIPL sublayer and MoCA scores in the inner retinal layer ($r=0.40, P<0.001$) and that between the OS sublayer and MoCA scores in the outer layer ($r=0.448, P<0.001$) (Fig. 4D).

Discussion

The purpose of this study is to investigate whether retinal metrics measured by OCT aid in the early screening and brain pathology monitoring for confirmed AD. To

our knowledge, the present work is the first to systematically compare retinal OCT-ISCF and thickness in different stages of AD. The primary finding of our study is that the outer retinal OCT-ISCF can significantly improve the discrimination performance between AD and CN compared to traditional retinal thickness parameters. Furthermore, the retinal OCT-ISCF present excellent repeatability and robust for early detection of AD using experimental and simulation methods. Finally, the retinal OCT-ISCF are more strongly correlated with AD pathological changes, including brain Aβ plaque burden and MoCA scores, than retinal thickness.

Firstly, retinal OCT-ISCF in the OS layer have changed in MCI, prior to the retinal thickness in our study. Several histopathological works confirmed that AD biomarkers are deposited in the outer retina, including OS layer, which lead to retinal neurodegeneration [7, 30]. Recently,

a study demonstrated that rod degeneration is the earliest AD retinal manifestations compared with cone and bipolar cells in AD mice [31]. The retinal MEZ sublayer thickness in the peripheral macular area in the ADD was significantly thinner than that in the CN. In addition, we also reported thickness thinning in the RNFL sublayer in ADD, consistent with previous studies [12, 32]. Interestingly, the trend of thickening in retinal RNFL sublayers existed in MCI, also reported by recent studies [10, 33]. Researchers attributed the retinal thickening at the MCI stage to glial cell proliferation prior to the retinal degeneration [34]. Considering the opposite effect of glial proliferation and neurodegeneration in retinal thickness, the high overlap between early AD and healthy individuals occurs, requiring more sensitivity retinal biomarkers for early AD detection. In nature, the retinal OCT-ISCF characterize the spatial correlation distribution of retinal OCT intensity signal, which is affected by tissular optical scattering property [35, 36]. Using the co-registered angle-resolved low-coherence interferometry OCT, Song et al. found that different retinal sublayers in AD mouse have alterations in tissue optical scattering signals, prior to retinal thickness changes. [37] However, the above technique adopted a complex structure design, making it difficult for clinical application. In contrast, we developed a radiomic analysis algorithm based on the OCT commercial device, and found that outer retinal OCT-ISCF alterations advanced to its thickness abnormality in clinical data. Using ROC analysis, the retinal OCT-ISCF showed higher accuracy than thickness parameters to distinguish CN with MCI and ADD. The results suggest that retinal OCT-ISCF may be a potential biomarker for the early screening of AD.

Secondly, the retinal OCT-ISCF are new indicators with excellent repeatability and robustness. The OCT-ISCF may be affected by light angles, refractive media, retinal disease and OCT speckle noise, etc. As we known, Henle's fiber layer presents a different appearance in OCT images under different light angles [38]. Thus, we instructed all subjects to maintain in primary position, avoiding the effect of light angles on OCT intensity. In the retinal OCT repeat experiments, the ICCs of all retinal OCT-ISCF were greater than 0.8, suggesting OCT-ISCF have good repeatability. Moreover, retinal OCT-ISCF significantly altered after cataract surgery. Therefore, our study matched retinal OCT image quality index to minimize the effects of refractive media opacity. In addition, we also excluded retinal diseases, thus reducing the influence of retinal diseases on the retinal OCT-ISCF. As for OCT speckle noise, we simulated speckle noise by randomly adding highlighted signals to the OS layer on OCT images. As a result, OCT-ISCF changed significantly after the addition of speckle noise. However,

the pattern of OCT-ISCF alterations by speckle noise was opposite to those caused by AD observed in this study. Overall, the retinal OCT-ISCF alterations seem to be associated with AD pathological changes, but not other relevant factors.

More importantly, the correlations between retinal OCT-ISCF and AD pathological changes are stronger than those in retinal thickness. The retinal OCT-ISCF alteration in AD may attribute to several reasons: Firstly, retinal A β plaques may contribute to the retinal OCT-ISCF alteration. Several studies conducted the retinal immunohistochemical analysis, and identified the presence of A β plaques in the retina [39, 40]. Using spectral imaging techniques, different groups have confirmed A β plaques cause changes in tissular optical scattering property, affecting the retinal OCT-ISCF [35, 41]. Considering the parallels in retina and brain pathophysiology of AD, we use brain A β plaque burden to indirectly represent retinal A β plaque burden. Previous studies reported that retinal thickness is linearly related to cerebral cortex SUVr value after controlling for any main effects of age, of which correlation coefficient is similar with our results [42, 43]. Of note, it's first time to report the retinal OCT-ISCF have middle correlations with brain A β plaque burden, which are stronger than thickness. From the A β deposition perspective, retinal OCT-ISCF better reflect pathological changes in AD when compared to the thickness. Secondly, neurodegeneration may also cause changes in OCT-ISCF. The cognitive impairment often represents brain neurodegeneration, therefore we analyze the correlation between retinal metrics and cognitive performance [44, 45]. Previously, several studies demonstrated that retinal thickness has a linear relationship with MoCA scores in AD, consistent with our finding. One interesting finding is retinal OCT-ISCF are more strongly correlated with MoCA scores than retinal thickness. Specifically, the Pearson's correlation coefficient of COR in GCIPL and RPE sublayers are 0.40, and 0.448, respectively. The above sublayers are the most common sites of retinal neurodegeneration [7, 46]. It is found that the optical density of RNFL in glaucoma patients is lower than that of normal subjects, and it gradually decreases with glaucoma progression, even before the thickness change [15]. In other words, retinal neurodegeneration is likely to cause the OCT-ISCF changes. Taken together, retinal OCT-ISCF have the potential to be used as an objective assessment of brain A β plaques burden and cognitive performance.

There are several limitations in our study. Firstly, the sample size is relatively small. Since there was no previous study to investigate OCT-ISCF parameters, we estimated sample sizes for the OCT-ISCF indicators with significant difference among groups in this study. For

example, for the ASM and COR parameters in the retinal OS layer, we calculated effect size of 0.714 and 0.976, respectively, based on the Cohen's formula [47]. Assuming alpha error and power of 0.05 and 0.8, respectively, the total sample sizes for the three groups could be calculated to be 24 and 15 using the G*power software, which are less than the actual included sample size of 82 in our study. As such, the current sample size in our study is sufficient to support the significant changes in retinal OCT-ISCF. Secondly, this study is cross-sectional. Although retinal metrics are associated with pathological alterations in AD, longitudinal data are still required to validate. Thirdly, we evaluate the refraction rather than ocular axial length. To some extent, spherical equivalent has a relationship with the ocular axial length, avoiding the effect of lateral magnification differences on the retinal metrics due to differences in ocular axial length. Finally, this study focuses on the research about AD and retinal metrics, which may be affected by ocular diseases and other neurodegenerative diseases. In the future, the retinal OCT-ISCF are necessary to be further validated in a general population.

Conclusions

The present study demonstrates that retinal OCT-ISCF significantly improve the association of pathological changes, including brain A β plaque burden and MoCA scores, and detection efficacy in AD compared to retinal thickness. In addition, a rigorous experimental design is used to clarify the excellent repeatability and robustness of retinal OCT-ISCF for AD screening and monitoring in clinical. These findings provide a theoretical basis for early screening and brain pathology monitoring in AD by using a combination of OCT and radiomic analysis methods, suggesting that retinal OCT-ISCF have the potential to be used as new biomarkers for AD.

Abbreviations

A β	Amyloid-beta
AD	Alzheimer's disease
ADD	AD-derived dementia
ASM	Angular second moment
AUC	Area under the curve
BCVA	Best corrected visual acuity
CDR	Clinic dementia rate
CN	Cognitive normal
COR	Correlation
CON	Contrast
CSF	Cerebrospinal fluid
DIS	Dissimilarity
ETDRS	Early treatment diabetic retinopathy study
GCL	Ganglion cell layer
GLCM	Gray-Level Co-occurrence Matrix
HOM	Homogeneity
ICC	Interclass correlation coefficient
INL	Inner nuclear layer
IOP	Intraocular pressure
IPL	Inner plexiform layer
MCI	Mild cognitive impairment

MEZ	Myoid and Ellipsoid zone
MoCA	Montreal Cognitive Assessment
OCT	Optical coherence tomography
OCT-ISCF	OCT intensity spatial correlation features
ONL	Outer nuclear layer
OPL	Outer plexiform layer
OS	Outer segment of photoreceptors
PET	Positron emission tomography
RNFL	Retinal nerve fiber layer
ROC	Receiver operating characteristics
RPE	Retinal pigment epithelial layer
SE	Spherical equivalent
SUVr	Standardised uptake value ratio

Supplementary Information

The online version contains supplementary material available at <https://doi.org/10.1186/s13195-025-01676-z>.

Additional file 1. eMethods. Detailed Methods. eTable 1. Characteristics of macular retinal sublayer thickness using ETDRS grid in CN, MCI, and ADD. eTable 2. Repeatability results of full-layer retinal OCT-ISCF parameters. eTable 3. Comparison of retinal OCT-ISCF among three groups. eFigure 1. Changes of OCT-ISCF before and after cataract surgery. (A-E) stands for CON, ASM, COR, HOM and DIS, respectively (Pre: Preoperative; Post: post-operative). eFigure 2. OCT-ISCF parameter change pattern of speckle noise signal in 5 normal subjects. (A-E) The results of CON, ASM, COR, HOM and DIS, respectively (CG: control group; TG: test group). eReferences.

Acknowledgements

We would like to thank Li Lei and Chengrong Tan for their assistance in the collection of subject data.

Authors' contributions

Z. Jin and X. Wang have full access to all research data in the paper and are responsible for the completeness and accuracy of the data analysis. Concept and Design: M. Shen, Y. Wang, Z. Jin, X. Wang. Data acquisition, analysis or interpretation: Z. Jin, X. Wang, S. Ye, H. Gao, Y. Lang, Y. Shen, G. Zeng, F. Zhou. Manuscript drafting: X. Wang. Critical revision of manuscripts with important intellectual content: M. Shen, Z. Jin. Statistical Analysis: Y. Song, H. Zhan, W. Shama. Instructors: F. Lu, M. Shen. All authors read and approved the final manuscript.

Funding

This work was supported by the Natural Science Foundation of China (No. 82301270, 82171016, U22A20312), Natural Science Foundation of Zhejiang Province China (Nos. LZ21F020008 and LY21A040001), Medical and Science & Technology Project of Zhejiang Province (2024KY162), Basic Research Program of Wenzhou Medical University (KYYW202302), and Major Scientific and Technological Innovation Project in Wenzhou (ZY2024018).

Data availability

The datasets used and/or analyzed during the current study are available from the corresponding author on reasonable request.

Declarations

Ethics approval and consent to participate

The study was approved by the Ethics Committee of the Third Affiliated Hospital of the PLA Army Medical University (Approval No. 2020-14) and the Affiliated Eye Hospital of Wenzhou Medical University (Approval No. 2020-012-K-10) in accordance with the principles of the Declaration of Helsinki, and written informed consent from all participants were obtained.

Competing interests

The authors declare no competing interests.

Author details

¹National Engineering Research Center of Ophthalmology and Optometry, Eye Hospital, Wenzhou Medical University, Wenzhou 325027, China. ²State Key Laboratory of Ophthalmology, Optometry and Vision Science, Eye Hospital, Wenzhou Medical University, Wenzhou 325027, China. ³National Clinical Research Center for Ocular Diseases, Eye Hospital, Wenzhou Medical University, Wenzhou 325027, China. ⁴Department of Neurology and Centre for Clinical Neuroscience, Daping Hospital, Third Military Medical University, Chongqing, China.

Received: 7 August 2024 Accepted: 15 January 2025

Published online: 01 February 2025

References

- Martínez G, Vernooij RW, Fuentes Padilla P, Zamora J, Flicker L, Bonfill Cosp X. 18F PET with flutemetamol for the early diagnosis of Alzheimer's disease dementia and other dementias in people with mild cognitive impairment (MCI). *Cochrane Database Syst Rev*. 2017;11(11):Cd012884. <https://doi.org/10.1002/14651858.Cd012884>
- Rabinovici GD, Gatzonis C, Apgar C, et al. Association of Amyloid Positron Emission Tomography With Subsequent Change in Clinical Management Among Medicare Beneficiaries With Mild Cognitive Impairment or Dementia. *JAMA*. 2019;321(13):1286–94. <https://doi.org/10.1001/jama.2019.2000>
- Sabbagh MN, Lue LF, Fayard D, Shi J. Increasing Precision of Clinical Diagnosis of Alzheimer's Disease Using a Combined Algorithm Incorporating Clinical and Novel Biomarker Data. *Neurol Ther*. 2017;6(Suppl 1):83–95. <https://doi.org/10.1007/s40120-017-0069-5>
- London A, Benhar I, Schwartz M. The retina as a window to the brain—from eye research to CNS disorders. *Nat Rev Neurol*. 2013;9(1):44–53. <https://doi.org/10.1038/nrneuro.2012.227>
- Sakata LM, Deleon-Ortega J, Sakata V, Kirkin CA. Optical coherence tomography of the retina and optic nerve - a review. *Clin Exp Ophthalmol*. 2009;37(1):90–9. <https://doi.org/10.1111/j.1442-9071.2009.02015.x>
- Cuenca N, Ortuño-Lizarán I, Sánchez-Sáez X, et al. Interpretation of OCT and OCTA images from a histological approach: Clinical and experimental implications. *Prog Retin Eye Res*. 2020;77: 100828. <https://doi.org/10.1016/j.preteyeres.2019.100828>
- Chan VTT, Sun Z, Tang S, et al. Spectral-Domain OCT Measurements in Alzheimer's Disease: A Systematic Review and Meta-analysis. *Ophthalmology*. 2019;126(4):497–510. <https://doi.org/10.1016/j.ophtha.2018.08.009>
- Casaleto KB, Ward ME, Baker NS, et al. Retinal thinning is uniquely associated with medial temporal lobe atrophy in neurologically normal older adults. *Neurobiol Aging*. 2017;51:141–7. <https://doi.org/10.1016/j.neurobiolaging.2016.12.011>
- Chen S, Zhang D, Zheng H, et al. The association between retina thinning and hippocampal atrophy in Alzheimer's disease and mild cognitive impairment: a meta-analysis and systematic review. *Front Aging Neurosci*. 2023;15:1232941. <https://doi.org/10.3389/fnagi.2023.1232941>
- Lad EM, Mukherjee D, Stinnett SS, et al. Evaluation of inner retinal layers as biomarkers in mild cognitive impairment to moderate Alzheimer's disease. *PLoS ONE*. 2018;13(2): e0192646. <https://doi.org/10.1371/journal.pone.0192646>
- Salobrar-García E, de Hoz R, Ramírez AI, et al. Changes in visual function and retinal structure in the progression of Alzheimer's disease. *PLoS ONE*. 2019;14(8): e0220535. <https://doi.org/10.1371/journal.pone.0220535>
- Ge YJ, Xu W, Ou YN, et al. Retinal biomarkers in Alzheimer's disease and mild cognitive impairment: A systematic review and meta-analysis. *Ageing Res Rev*. 2021;69: 101361. <https://doi.org/10.1016/j.arr.2021.101361>
- Hadoux X, Hui F, Lim JKH, et al. Non-invasive in vivo hyperspectral imaging of the retina for potential biomarker use in Alzheimer's disease. *Nat Commun*. 2019;10(1):4227. <https://doi.org/10.1038/s41467-019-12242-1>
- Lemmens S, Van Eijgen J, Van Keer K, et al. Hyperspectral Imaging and the Retina: Worth the Wave? *Transl Vis Sci Technol*. 2020;9(9):9. <https://doi.org/10.1167/tvst.9.9.9>
- Huang XR, Zhou Y, Kong W, Knighton RW. Reflectance decreases before thickness changes in the retinal nerve fiber layer in glaucomatous retinas. *Invest Ophthalmol Vis Sci*. 2011;52(9):6737–42. <https://doi.org/10.1167/iov.11-7665>
- Villemagne VL, Burnham S, Bourgeat P, et al. Amyloid β deposition, neurodegeneration, and cognitive decline in sporadic Alzheimer's disease: a prospective cohort study. *Lancet Neurol*. 2013;12(4):357–67. [https://doi.org/10.1016/s1474-4422\(13\)70044-9](https://doi.org/10.1016/s1474-4422(13)70044-9)
- Stetson PF, Yehoshua Z, Garcia Filho CA, Portella Nunes R, Gregori G, Rosenfeld PJ. OCT minimum intensity as a predictor of geographic atrophy enlargement. *Invest Ophthalmol Vis Sci*. 2014;55(2):792–800. <https://doi.org/10.1167/iov.13-13199>
- Chen H, Xia H, Qiu Z, Chen W, Chen X. CORRELATION OF OPTICAL INTENSITY ON OPTICAL COHERENCE TOMOGRAPHY AND VISUAL OUTCOME IN CENTRAL RETINAL ARTERY OCCLUSION. *Retina*. 2016;36(10):1964–70. <https://doi.org/10.1097/iae.0000000000001017>
- Schmitt JM, Knüttel A, Bonner RF. Measurement of optical properties of biological tissues by low-coherence reflectometry. *Appl Opt*. 1993;32(30):6032–42. <https://doi.org/10.1364/ao.32.006032>
- Koronyo Y, Biggs D, Barron E, et al. Retinal amyloid pathology and proof-of-concept imaging trial in Alzheimer's disease. *JCI Insight*. 2017;2(16). <https://doi.org/10.1172/jci.insight.93621>
- Depeursinge A, Foncubierta-Rodriguez A, Van De Ville D, Müller H. Three-dimensional solid texture analysis in biomedical imaging: review and opportunities. *Med Image Anal*. 2014;18(1):176–96. <https://doi.org/10.1016/j.media.2013.10.005>
- Elsharkawy M, Sharafeldeen A, Soliman A, et al. A Novel Computer-Aided Diagnostic System for Early Detection of Diabetic Retinopathy Using 3D-OCT Higher-Order Spatial Appearance Model. *Diagnostics (Basel)*. 2022;12(2). <https://doi.org/10.3390/diagnostics12020461>
- Petersen RC, Doody R, Kurz A, et al. Current concepts in mild cognitive impairment. *Arch Neurol*. 2001;58(12):1985–92. <https://doi.org/10.1001/archneur.58.12.1985>
- Liu X, Shen M, Yuan Y, et al. Macular Thickness Profiles of Intraretinal Layers in Myopia Evaluated by Ultrahigh-Resolution Optical Coherence Tomography. *Am J Ophthalmol*. 2015;160(1):53–61.e52. <https://doi.org/10.1016/j.ajpo.2015.03.012>
- Staurinchi G, Sadda S, Chakravarthy U, Spaide RF. Proposed lexicon for anatomic landmarks in normal posterior segment spectral-domain optical coherence tomography: the IN-OCT consensus. *Ophthalmology*. 2014;121(8):1572–8. <https://doi.org/10.1016/j.ophtha.2014.02.023>
- Sharafeldeen A, Elsharkawy M, Khalifa F, et al. Precise higher-order reflectivity and morphology models for early diagnosis of diabetic retinopathy using OCT images. *Sci Rep*. 2021;11(1):4730. <https://doi.org/10.1038/s41598-021-83735-7>
- Gao W, Lin P, Li B, et al. Quantitative assessment of textural features in the early detection of diabetic retinopathy with optical coherence tomography angiography. *Photodiagnosis Photodyn Ther*. 2023;41: 103214. <https://doi.org/10.1016/j.pdpdt.2022.103214>
- Zhou Y, Yu K, Wang M, et al. Speckle Noise Reduction for OCT Images Based on Image Style Transfer and Conditional GAN. *IEEE J Biomed Health Inform*. 2022;26(1):139–50. <https://doi.org/10.1109/jbhi.2021.3074852>
- Yan Q, Chen B, Hu Y, et al. Speckle reduction of OCT via super resolution reconstruction and its application on retinal layer segmentation. *Artif Intell Med*. 2020;106: 101871. <https://doi.org/10.1016/j.artmed.2020.101871>
- den Haan J, Verbraak FD, Visser PJ, Bouwman FH. Retinal thickness in Alzheimer's disease: A systematic review and meta-analysis. *Alzheimers Dement (Amst)*. 2017;6:162–70. <https://doi.org/10.1016/j.dadm.2016.12.014>
- Zhang J, Gao F, Ma Y, Xue T, Shen Y. Identification of early-onset photoreceptor degeneration in transgenic mouse models of Alzheimer's disease. *iScience*. 2021;24(11):103327. <https://doi.org/10.1016/j.isci.2021.103327>
- Ferrari L, Huang SC, Magnani G, Ambrosi A, Comi G, Leocani L. Optical Coherence Tomography Reveals Retinal Neuroaxonal Thinning in Frontotemporal Dementia as in Alzheimer's Disease. *J Alzheimers Dis*. 2017;56(3):1101–7. <https://doi.org/10.3233/JAD-160886>
- Ascaso FJ, Cruz N, Modrego PJ, et al. Retinal alterations in mild cognitive impairment and Alzheimer's disease: an optical coherence tomography study. *J Neurol*. 2014;261(8):1522–30. <https://doi.org/10.1007/s00415-014-7374-z>

34. Salobrar-García E, Rodrigues-Neves AC, Ramírez AI, et al. Microglial Activation in the Retina of a Triple-Transgenic Alzheimer's Disease Mouse Model (3xTg-AD). *Int J Mol Sci.* 2020;21(3). <https://doi.org/10.3390/ijms21030816>
35. More SS, Beach JM, McClelland C. In Vivo Assessment of Retinal Biomarkers by Hyperspectral Imaging: Early Detection of Alzheimer's Disease. *ACS Chem Neurosci.* 2019;10(11):4492–501. <https://doi.org/10.1021/acscchemneuro.9b00331>.
36. More SS, Beach JM, Vince R. Early Detection of Amyloidopathy in Alzheimer's Mice by Hyperspectral Endoscopy. *Invest Ophthalmol Vis Sci.* 2016;57(7):3231–8. <https://doi.org/10.1167/iovs.15-17406>.
37. Song G, Steelman ZA, Finkelstein S, et al. Multimodal Coherent Imaging of Retinal Biomarkers of Alzheimer's Disease in a Mouse Model. *Sci Rep.* 2020;10(1):7912. <https://doi.org/10.1038/s41598-020-64827-2>.
38. Russell DJ, Fallah S, Loer CJ, Riffenburgh RH. A comprehensive model for correcting RNFL readings of varying signal strengths in cirrus optical coherence tomography. *Invest Ophthalmol Vis Sci.* 2014;55(11):7297–302. <https://doi.org/10.1167/iovs.14-14993>.
39. Koronyo-Hamaoui M, Koronyo Y, Ljubimov AV, et al. Identification of amyloid plaques in retinas from Alzheimer's patients and noninvasive in vivo optical imaging of retinal plaques in a mouse model. *Neuroimage.* 2011;54(Suppl 1):S204–217. <https://doi.org/10.1016/j.neuroimage.2010.06.020>.
40. Shi H, Koronyo Y, Rentsendorj A, et al. Identification of early pericyte loss and vascular amyloidosis in Alzheimer's disease retina. *Acta Neuropathol.* 2020;139(5):813–36. <https://doi.org/10.1007/s00401-020-02134-w>.
41. Lemmens S, Van Craenendonck T, Van Eijgen J, et al. Combination of snapshot hyperspectral retinal imaging and optical coherence tomography to identify Alzheimer's disease patients. *Alzheimers Res Ther.* 2020;12(1):144. <https://doi.org/10.1186/s13195-020-00715-1>.
42. Santos CY, Johnson LN, Sinoff SE, Festa EK, Heindel WC, Snyder PJ. Change in retinal structural anatomy during the preclinical stage of Alzheimer's disease. *Alzheimers Dement (Amst).* 2018;10:196–209. <https://doi.org/10.1016/j.dadm.2018.01.003>.
43. Marquié M, Valero S, Castilla-Martí M, et al. Association between retinal thickness and β -amyloid brain accumulation in individuals with subjective cognitive decline: Fundació ACE Healthy Brain Initiative. *Alzheimers Res Ther.* 2020;12(1):37. <https://doi.org/10.1186/s13195-020-00602-9>.
44. Kim HM, Han JW, Park YJ, Bae JB, Woo SJ, Kim KW. Association Between Retinal Layer Thickness and Cognitive Decline in Older Adults. *JAMA Ophthalmol.* 2022;140(7):683–90. <https://doi.org/10.1001/jamaophth.2022.1563>.
45. Cunha LP, Lopes LC, Costa-Cunha LV, et al. Macular Thickness Measurements with Frequency Domain-OCT for Quantification of Retinal Neural Loss and its Correlation with Cognitive Impairment in Alzheimer's Disease. *PLoS ONE.* 2016;11(4): e0153830. <https://doi.org/10.1371/journal.pone.0153830>.
46. Bruban J, Glotin AL, Dinét V, et al. Amyloid-beta(1–42) alters structure and function of retinal pigmented epithelial cells. *Aging Cell.* 2009;8(2):162–77. <https://doi.org/10.1111/j.1474-9726.2009.00456.x>.
47. Cohen J. *Statistical Power Analysis for the Behavioral Sciences.* 2nd Edition. In: Lawrence Erlbaum Associates. 1988. p. 20–21. <https://doi.org/10.4324/9780203771587>.

Publisher's Note

Springer Nature remains neutral with regard to jurisdictional claims in published maps and institutional affiliations.